THE JOURNAL OF PHYSICAL CHEMISTRY C

ARTICLE

pubs.acs.org/JPCC

Encapsulating a Ternary Europium Complex in a Silica/Polymer Hybrid Matrix for High Performance Luminescence Application

Xiaoguang Huang, Qin Wang, Xuhuan Yan, Jun Xu, Weisheng Liu, Qing Wang, and Yu Tang*

Key Laboratory of Nonferrous Metal Chemistry and Resources Utilization of Gansu Province, State Key Laboratory of Applied Organic Chemistry, College of Chemistry and Chemical Engineering, Lanzhou University, Lanzhou 730000, People's Republic of China

Supporting Information

ABSTRACT: The sol−gel method has been proven to be an excellent approach for the preparation of hybrid materials. Combining luminescent lanthanide complexes with silica/polymer hybrid materials to improve the stability and even to increase luminescent properties is fascinating and promising in the lanthanide complex hybrid material field. A series of tough and transparent hybrid materials polymer−Eu−L−P gel have been assembled by a ternary europium complex $[Eu_2L_2(Phen)_2(CH_3OH)_4]Cl_2 \cdot (CH_3OH)_6$($H_2L$ = 2,2′-(((2,4,6-trimethyl-1,3-phenylene)bis(methylene))bis(oxy))dibenzoic acid, Phen =1,10-phenanthroline) embedded into microporous silica/polymer [poly(methyl methacrylate) (PMMA), polyvinylpyrrolidone (PVP), and poly(vinyl butyral) (PVB)] matrixes. The Fourier transform infrared (FTIR) spectra, UV−vis absorption spectra, X-ray diffraction (XRD), scanning electronic microstructure (SEM), thermogravimetry (TG), and luminescent properties of the europium ternary complex and the hybrid materials (Eu−L−P gel and polymer−Eu−L−P gel) are described in detail. The hybrid materials polymer−Eu−L−P gel display more efficient unit mass luminescence emission, longer lifetime, higher quantum efficiency, greater thermal stability, and better exposure durability in comparison with the Eu−L−P gel. The result may support the conclusion that the polymers could interact with the complex, act as antennae, and transfer energy to the central Eu^{3+} ions. Comparatively, diminutive distinction exists in the hybrid materials containing different polymers originated from the weak interactions between the host and the guest.

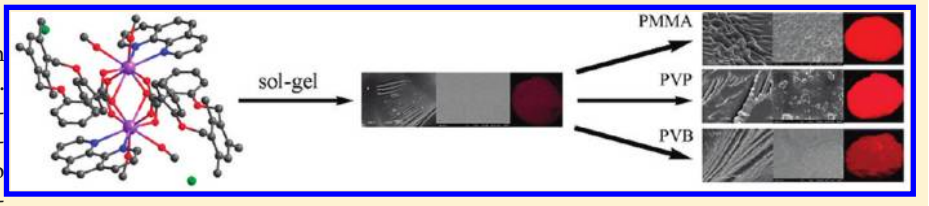

INTRODUCTION

Lanthanide ions have characteristic and narrow emission bands based on their f−f electronic transitions and a wide range of luminescence lifetimes, suitable for various applications such as chemosensors, and as probes and labels in a variety of biological and chemical devices.[1,2] However, the application of lanthanide-based luminescence suffers from two serious drawbacks: (1) low absorption coefficients because of the f−f electronic transitions which are forbidden and (2) efficient nonradiative deactivation of their excited states by O−H oscillators such as water. For the sake of avoiding these obvious problems for the application of lanthanides, a strategy has been developed that involves the so-called antenna effect.[3,4] In order to further optimize the light output and decrease the internal nonradiative decay processes, the chromophoric ligands which chelate to lanthanide metals should be able (1) to absorb and transfer energy efficiently to the central metal and (2) to encapsulate and protect the lanthanide ion from the solvent molecules.[5,6] Podand-type ligands have been dramatically concentrated on due mainly to their selective coordinating capacities, spheroidal cavities, and hard binding sites stabilizing complexes, acquiring novel coordination structures and shielding the encapsulated ions from interaction with the surroundings.[6−10] In addition, noncharged ligands such as 1,10-phenanthroline can serve as synergistic agents, since a vital issue about the design of lanthanide complexes is to prevent water molecules from binding to the lanthanide ions.

However, lanthanide complex solids are difficult to directly utilize as luminescent sources because of poor thermal resistivity, weak moisture stability, and feeble mechanical strength. The problems are expected to be solved by encapsulating or adsorbing the complexes in suitable solid matrixes including polymers,[11,12] sol−gel silica[2,13] or organically modified silicates (ORMOSIL),[13−15] zeolites,[16] mesoporous materials,[4,17] TiO_2[18] or α-ZrP,[19] liquid crystals,[3,20] and even carbon nanotubes[21] or clays.[22] As the existing literature illustrates, the hybrid materials doped with lanthanide complexes possess characteristic luminescent properties including the sharp, intense emission bands based on f−f electronic transitions and a wide range of lifetimes, which are suitable for various applications.[23,24]

To date, among all the synthetic methods, based on hydrolysis/polycondensation reactions, sol−gel technology derived from hybrid materials has received great interest and has been considered as an excellent approach for the preparation of novel

Received: August 5, 2010
Revised: December 5, 2010
Published: January 12, 2011

hybrid materials at a temperature lower than those of the conventional method.[25,26] As a result of its relatively low temperature processing, active species such as lanthanide organic complexes can be incorporated into host matrixes (inorganic or organic polymer matrixes), and the obtained hybrid materials exhibit improved processability, boosted chemical stability, and enhanced mechanical strength.[27] Additionally, this mild synthetic method allows the hybrids to exhibit high versatility and offers a wide range of chances for preparation of tailor-made materials in terms of their unique features. In particular, the prominent advantage of sol−gel technology is that the microstructure, external shape, and degree of combination between the two phases can be controlled by altering the sol−gel processing conditions.[28] However, conventional gels tend to crack during the drying period owing to their poor mechanical strength. What is more, the SiO_2 matrix containing −OH can extensively reduce luminescence emission intensity and decay time.[29] In order to solve the problems, one of the best strategies is to introduce a polymer into a silica matrix, which allows for increasing the solubility of complexes in the sol−gel matrix while variation of the percentage of the silica/polymer components allows for modification of both mechanical and optical properties of the materials.[30−32] Employing organic polymer leads to the reduction or virtual suppression of groups responsible for luminescence quenching, and can also solve the problem of clustering of emitting centers because only weak interactions (such as hydrogen bonding, van der Waals forces, or weak static effects) exist between organic and inorganic moieties.

In order to enhance the luminescent properties and improve the stability of the lanthanide complex and discuss the effects of the interaction between the host and guest molecules on the properties, herein we attempted to assemble novel ternary europium complex silica/polymer hybrid luminescent materials, using the podand-type ligand 2,2′-(((2,4,6-trimethyl-1,3-phenylene)bis(methylene))bis(oxy))dibenzoic acid (L) to immobilize europium ion for the first time and noncharged ligand 1,10-phenanthroline to enhance the luminescent properties. Remarkably, the most studied various lighting applications are conceivable by using Eu^{3+}, Tb^{3+}, Dy^{3+}, and Sm^{3+}, along with suitable antennas, blended in stable and transparent inorganic hosts. Via the emission spectrum, the radiative lifetime of the Eu^{3+} ion can be directly calculated, which had been more briefly addressed than those of other Ln^{3+} ions. The chemical structures of the employing organic polymers (poly(methyl methacrylate) (PMMA), polyvinylpyrrolidone (PVP), and poly(vinyl butyral) (PVB)) are shown in Figure 1. As illustrated in Figure 1, we can clearly see that PMMA, PVP, and PVB have carbonyl groups, which may be coordinated with the central lanthanide ions and considerably enhance the luminescent properties of the hybrid materials. PVB is commercially prepared by a well-known reaction between aldehydes and alcohols.[33] However, the resulting polymer is actually a terpolymer of PVB, poly(vinyl alcohol) (PVA), and poly(vinyl acetate) because of incomplete conversion, and it possesses hydroxyl groups in the chain which may influence the luminescence intensity of the hybrid material.

EXPERIMENTAL SECTION

Materials. Europium chloride ($EuCl_3 \cdot 6H_2O$) was obtained by dissolving Eu_2O_3 (99.99%, Shanghai Yuelong) in hydrochloric acid followed by successive fuming to remove excess acid. 2,4-Bis(bromomethyl)-1,3,5-trimethylbenzene was prepared according to literature methods.[34] Tetraethoxysilane (TEOS), 1,10-phenanthroline

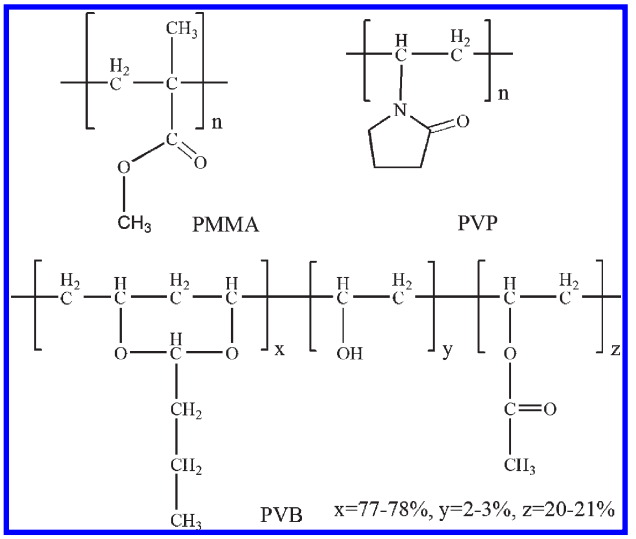

Figure 1. Chemical structures of commercial polymers PMMA, PVP, and PVB.

(Phen), and other chemicals were all commercially available and used without further purification.

Synthesis of 2,2′-(((2,4,6-Trimethyl-1,3-phenylene)bis(methylene))bis(oxy))dibenzoic Acid (H_2L). 2,4-Bis(bromomethyl)-1,3,5-trimethylbenzene (673 mg, 2.2 mmol), and salicylic acid (761 mg, 5.0 mmol) were added to acetone (25 cm^3), and then anhydrous potassium carbonate (690 mg, 5.0 mmol) was added. The reaction mixture was stirred and refluxed for 8 h. The reaction mixture was then poured into water, and the resulting precipitate was filtered off, washed with water, and dried. The resulting white solid (449 mg, 1.0 mmol) and sodium hydroxide (120 mg, 3.0 mmol) were added to the mixed solution of methanol (25 cm^3) and water (5 cm^3). The reaction mixture was stirred and refluxed for 3 h and then filtered, and hydrochloric acid was added (1.0 $mol \cdot dm^{-3}$) until no precipitate separated out. The precipitate was filtered and washed with water, until the pH of the washing solution was in the range 6−7, and dried at 60 °C. NMR data are available in the Supporting Information.

Synthesis of the Eu(III) Ternary Complex Eu−L−P. H_2L (420 mg, 1.0 mmol), Phen (198 mg, 1.0 mmol), and $EuCl_3 \cdot 6H_2O$ (366 mg, 1.0 mmol) were dissolved in a suitable volume of methanol at 40 °C. The pH value of the solution was adjusted by adding ammonia solution until a sediment was observed. The mixture was continually stirred for 3 h at room temperature and then allowed to stand overnight. The reactive solution was filtered, and the precipitate was washed with methanol and dried in a vacuum. Yield: 649 mg (63%). Elemental analysis (%) calcd (found) for $C_{78}H_{76}N_4O_{16}Cl_2Eu_2$: C, 55.07 (55.23); H, 4.48 (4.51); N, 3.63 (3.30). White block crystals suitable for X-ray single-crystal structural determination were grown from the mother liquor at room temperature.

Synthesis of Eu−L−P Gel. TEOS was first mixed with ethanol, and then HCl-acidified water (pH 2) was added to the above mixture under magnetic stirring to initiate the hydrolysis and condensation reaction. The molar ratio of TEOS/ethanol/H_2O was 1:4:4. A transparent sol was obtained. After stirring for 3 h, *N*,*N*-dimethylformamide (DMF) solution containing an appropriate amount of the ternary complex Eu−L−P (the mass ratio of Eu−L−P/SiO_2 was 3:10) was added to the sol. The mixture was stirred at room temperature for 4 h. The transparent gel was allowed to stand for 3 days and then dried at 373 K.

The gel was collected as monolithic bulks and ground into powdered material for the photophysical studies.

Synthesis of Polymer−Eu−L−P Gel (Polymer = PMMA, PVB, PVP). In a typical run, TEOS was first mixed with ethanol. Then HCl-acidified water (pH 2) was added to the above mixture under magnetic stirring to initiate the hydrolysis and condensation reaction. The molar ratio of TEOS/ethanol/H_2O was 1:4:4. After stirring for 3 h, DMF solutions containing the complex Eu−L−P and polymer were added to the sol. The mass ratio of Eu−L−P/PMMA/SiO_2 was 3:4:10. The mixture was stirred for 4 h at room temperature to ensure homogeneous mixing and complete hydrolysis, and then placed in a sealed container, which was kept at 45 °C until the precursor solution was converted into a transparent monolithic gel and ground into powdered material for the photophysical studies.

Physical Measurements. ^{1}H and ^{13}C NMR spectra were recorded on a Bruker 400 MHz spectrometer. Chemical shifts (δ) are given in parts per million (ppm), and coupling constants (J) are given in hertz (Hz). CHN elemental analyses were measured on an Elementar Vario EL analyzer. Fourier transform infrared (FTIR) spectra were conducted within the 4000−400 cm^{-1} wavenumber range using a Nicolet 360 FTIR spectrometer with the KBr pellet technique. Scanning electron microscope (SEM) images were taken on a JEM-5600 LV apparatus and a JSM-6701F apparatus. X-ray diffraction (XRD) patterns were determined with Rigaku-Dmax 2400 diffractometer using Cu Kα radiation over the 2θ range of 5−70°. The UV−vis absorption spectra were recorded on a Perkin-Elmer Lambda 950 spectrophotometer. Thermogravimetric (TG) analysis was performed on a Perkin-Elmer thermal analyzer up to 800 °C at a heating rate of 5 °C/min under air. The steady-state luminescence spectra and the lifetime measurements were measured on an Edinburgh Instruments FSL920 fluorescence spectrometer, with a 450 W Xe arc lamp as the steady-state excitation source or a Nd-pumped OPOlette laser as the excitation source for lifetime measurements; in the experiments of photoluminescence stability, monochromic light (347 nm) separated from the 450 W Xe arc lamp was used as the irradiation source, with a slit of 0.8 nm and a shutter opening after 10 s for 800 s.

Single-crystal X-ray diffraction measurements were carried out on a Bruker SMART 1000 CCD diffractometer operating at 50 kV and 30 mA using Mo Kα radiation (λ = 0.710 73 Å). The crystal was mounted inside a Lindemann glass capillary for data collection using SMART and SAINT software.[35,36] An empirical absorption correction was applied using the SADABS program.[37] The structure was solved by direct methods and refined by full-matrix least squares on F^2 using the SHELXTL-97 program package.[38] Primary non-hydrogen atoms were solved by direct method, and secondary non-hydrogen atoms were solved by difference maps. The hydrogen atoms were added geometrically and not refined. All calculations were performed using the programs SHELXS-97 and SHELXL-97.

Crystal data and structure determination details of the complex $[Eu_2L_2(Phen)_2(CH_3OH)_4]Cl_2\cdot(CH_3OH)_6$ are summarized in Table S1 in the Supporting Information.

RESULTS AND DISCUSSION

Crystal Structure of the Ternary Complex Eu−L−P. The solid state structure of the europium complex $[Eu_2L_2(Phen)_2(CH_3OH)_4]Cl_2\cdot(CH_3OH)_6$ (Eu−L−P) was determined by single-crystal X-ray diffraction. The molecular structure of the complex Eu−L−P and the coordination polyhedron of the central Eu^{3+} ion are depicted in Figure 2. The single-crystal X-ray analysis of the ternary complex reveals that the crystal crystallizes in the triclinic space group $P\bar{1}$ and consists of homodinuclear species in which the two Eu^{3+} ions are bridged by five oxygen atoms from two carboxylate ligands in different coordination modes. It is interesting to note that the dimeric structure of the Eu−L−P complex possesses an inversion center of symmetry, thus indicating that the two Eu(III) centers reside in equivalent chemical environments. The coordination sphere of the central Eu^{3+} ion can be described best as a distorted $[EuO_7N_2]$ tricapped triprism (Figure 2B), in which five oxygen atoms are provided by two bridging carboxylate ligands, two nitrogen atoms come from chelating Phen, and two oxygen atoms are furnished by two methanol molecules. The distance between the two central cations in the complex is 3.9795(3) Å. In the complex, the ligand L exhibits two different coordination modes to the Eu^{3+} ions (Figure 3), namely, two η^1-carboxylate interactions from the bridging benzoate groups and two bidentate chelating with an oxygen atom bridging two metal ions and another oxygen atom coordinating to one of the ions (triply coordinated, η^2-η^1-chelating benzoate groups). We may deduce that the carbonyl groups involved in the polymers may possibly participate in the coordination with the central Eu^{3+} ions in the hybrid materials, due to the unsaturated coordination number of the Eu^{3+} ions.

Characterization of Microstructure. The FTIR spectra of the materials Eu−L−P gel and PMMA−Eu−L−P gel are displayed in Figure 4, and the spectra of PVP−Eu−L−P gel and PVB−Eu−L−P gel are shown in Figure S1 in the Supporting Information. Herein only the spectra of Eu−L−P gel and PMMA−Eu−L−P gel will be described in detail. It is of little possibility to predict the forms of the complexes in Eu−L−P gel via the FTIR spectra, because of the low amount of Eu−L−P complexes incorporated in the matrix, and consequently the domination of the strong Si−O−Si framework vibrations (ν_{as}(Si−O) at ∼1050 cm^{-1} and δ(Si−O−Si) at ∼456 cm^{-1}) exist in Eu−L−P gel, which is attributed to the success of hydrolysis and copolycondensation reactions. An obvious shift of the Si−O−Si framework, which is evidenced by the vibrations ν_{as}(Si−O) (from 1050 to 1067 cm^{-1}) and δ(Si−O−Si) (from 456 to 446 cm^{-1}) can be observed in the spectra of the materials Eu−L−P gel and PMMA−Eu−L−P gel. The absorption band at 1655 cm^{-1} for the Eu−L−P gel can be assigned to the vibration of C═O groups of the ligands, whereas for the PMMA−Eu−L−P gel, it shifts to 1658 cm^{-1}. The results suggest the proper incorporation of the polymer into the hybrid material and may bring on small changes in the system via coordinating with the central Eu^{3+} ions.

The room-temperature X-ray diffraction patterns from 5 to 70° of the hybrid materials are shown in Figure 5, exhibiting that the obtained hybrid materials are amorphous in a wide region. The broad peaks centered about 23.88° and 3.723 Å (the structural unit distance calculated by using the Bragg law) for Eu−L−P gel, 22.30° and 3.983 Å for PMMA−Eu−L−P gel, 23.01° and 3.857 Å for PVP−Eu−L−P gel, and 23.04° and 3.863 Å for PVB−Eu−L−P gel can be attributed to the amorphous siliceous backbone of the hybrids.[39] The absence of any crystalline regions in these materials correlates with the presence of host inorganic networks. Moreover, we know the organic ligand and polymer are essentially in an ordered arrangement, while as seen from the diffractograms, the regular arrangements have been distorted in the final hybrid materials because the siliceous backbones belong to the inorganic region and possess less orderliness. The hybrid materials still hold disordered sequences even after the polymers have been doped, and the existence of

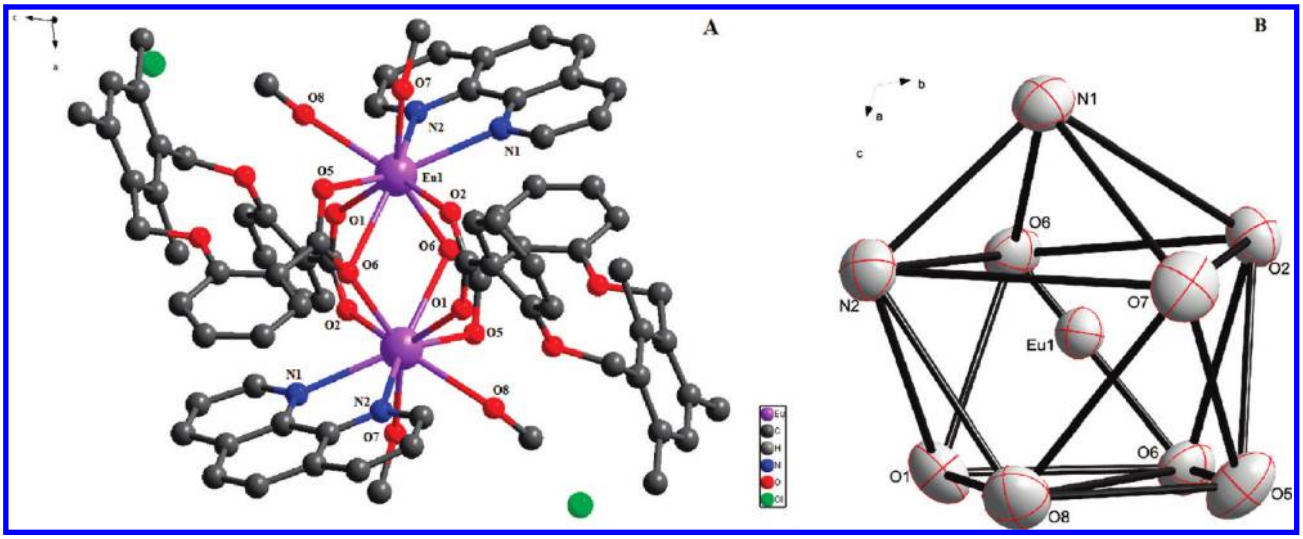

Figure 2. Structure of Eu−L−P showing the coordination sphere of Eu^{3+} (A, hydrogen atoms and crystal methanol molecules omitted for clarity) and coordination polyhedron of Eu^{3+} ion (B).

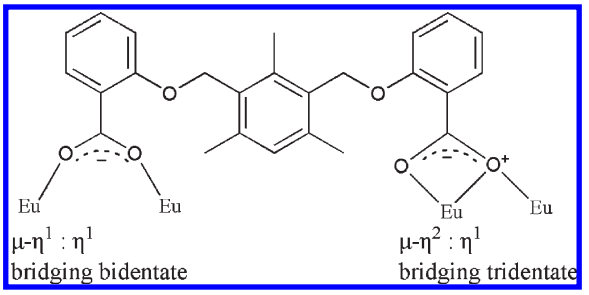

Figure 3. Different types of binding modes for the bridging ligand L observed in Eu−L−P.

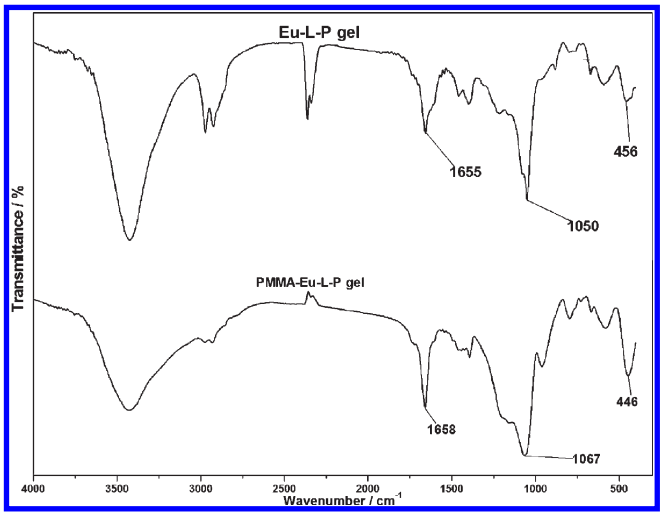

Figure 4. FTIR spectra of Eu−L−P gel and PMMA−Eu−L−P gel.

polymers did not decrease the overall disorder of the siliceous skeleton seen from the data, although polymeric carbons chains of the polymers are essentially regularly ordered.

The scanning electron micrographs of the representative lanthanide hybrid materials demonstrate that the skin-wrinkling materials were obtained (Figure 6, in the order Eu−L−P gel, PMMA−Eu−L−P gel, PVP−Eu−L−P gel, and PVB−Eu−L−P gel). The

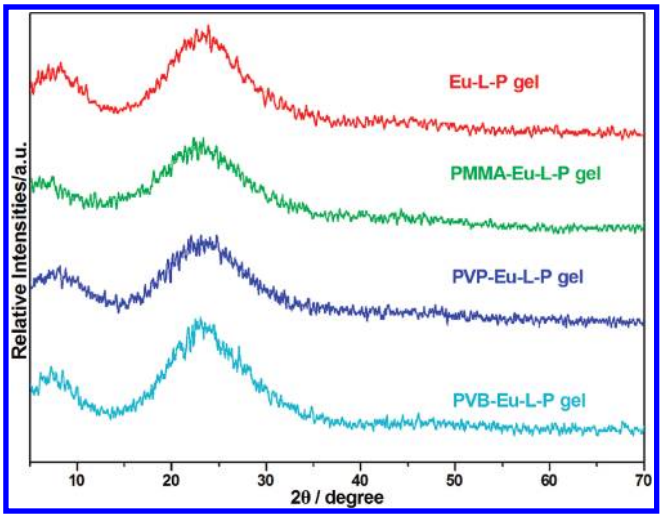

Figure 5. X-ray diffraction patterns for the hybrid materials: Eu−L−P gel, PMMA−Eu−L−P gel, PVP−Eu−L−P gel, and PVB−Eu−L−P gel.

micrographs in Figure 6, left, have been obtained on a JEM-5600 LV apparatus, and those in Figure 6, right, have been taken using a JSM-6701F apparatus. Different compositions have only a little influence on the micromorphology. On the surfaces of these materials, it is quite clear that the materials seem homogeneous and their surfaces display microporous structures. There are many linear stripes on the surface, which result from the sol−gel treatment. In the gelation process, the lanthanide complexes and polymers are ready to form three-dimensional network-like structures which will compete with the construction of the polymeric network structure of Si−O−Si in the hydrolysis and copolycondensation processes. Therefore, both tendencies have respective influence on the formation of the obtained hybrid polymeric materials. Moreover, rudimental solutions were released from inside the gel, leading to the final micromorphology. Because the foundation shrinks homogeneously, the skin of the material takes on a regular morphology. It is also proof that no phase separation occurs.

Luminescent Properties Analyses for the Hybrid Materials. *Absorption and Luminescence Spectra.* Aromatic carboxylic

dx.doi.org/10.1021/jp109644j |J. Phys. Chem. C 2011, 115, 2332–2340

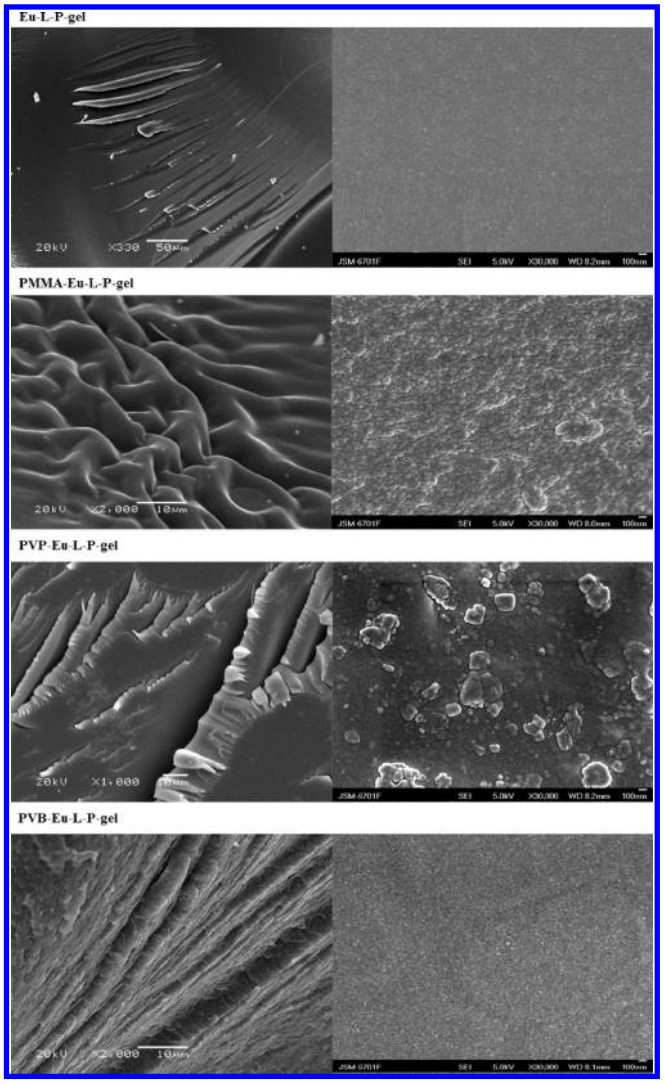

Figure 6. SEM images of the hybrid materials.

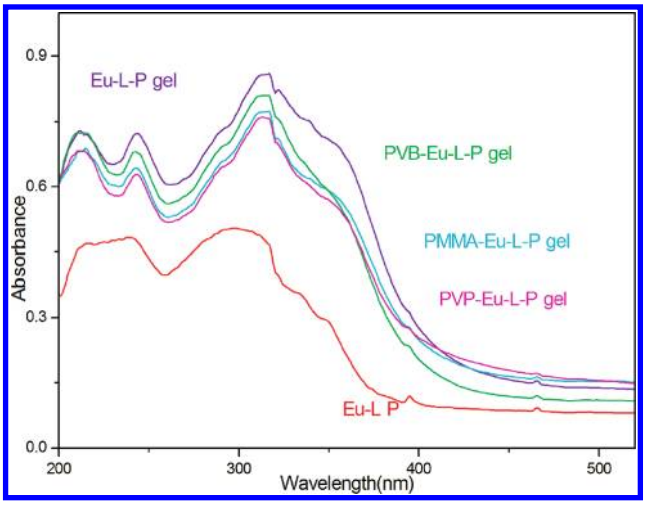

Figure 7. UV−vis absorption spectra of the solid samples.

acids are already well-known to be good chelating groups to sensitize the luminescence of lanthanide ions.[40] The solid state absorption spectra of the complex Eu−L−P and the hybrid materials Eu−L−P gel and polymer−Eu−L−P gel samples are displayed in Figure 7. Compared to Eu−L−P, a red shift of the major $\pi-\pi^*$ electronic transitions (from 305 to ~312 nm) occurs in Eu−L−P gel and polymer−Eu−L−P gel and a few changes on the peak shapes are apparent, which indicates that the electron distributions of the systems have changed when the complexes are embedded in the matrixes and the perturbation is induced by the silanol groups in the hybrid materials. The spectral shapes of the complex in polymer−Eu−L−P gel are a bit different from that of the Eu−L−P gel, suggesting the influence of the coordination of the carbonyl groups of the polymers with central Eu^{3+} ions. The determined molar absorption coefficient values of the materials at 312 nm are about 2 times higher than that of the pure complex, which reveals the matrixes may have strong abilities to assist the europium complex in absorbing light.

The excitation (left) and emission (right) spectra of polymer−Eu−L−P gel and isolated Eu^{3+} complex as solids at room temperature are illustrated in Figure 8. The excitation spectra of all samples, which were obtained by monitoring at 615 nm, exhibit a broad excitation band (BEB) between 250 and 450 nm. The broad excitation band can be assigned to the $\pi-\pi^*$ electron transition of the ligands, i.e., Phen and L. The peak observed at 395 nm in the excitation spectrum of Eu−L−P (Figure 8B) can be ascribed to the f−f transition ($^7F_0 \rightarrow {}^5L_6$) of Eu^{3+} ion. The weaker f−f transitions in comparison with the ligand absorption are overlapped by BEB, proving that luminescence sensitization via excitation of the ligands is more efficient than the direct excitation of the absorption levels of Eu^{3+} ions. In the emission spectra of all samples, only characteristic emissions of Eu^{3+} ions are detected, which indicates that the energy transfer from ligands to central Eu^{3+} ions (antenna effect) seems very efficient.[41] All samples showed characteristic narrow band emissions of Eu^{3+} corresponding to the $^5D_0 \rightarrow {}^7F_J$ ($J = 0-4$) transitions. The five expected peaks of the luminescence spectra throughout the $^5D_0 \rightarrow {}^7F_{0-4}$ transition regions are well resolved. The emission bands at 580 and 650 nm are very weak since their corresponding transitions $^5D_0 \rightarrow {}^7F_{0,3}$ are forbidden in both magnetic- and electric-dipole schemes.[42] The intensity of the emission band at 593 nm is relatively strong and independent of the coordination environment because of the magnetic-dipole $^5D_0 \rightarrow {}^7F_1$ transition; on the contrary, the $^5D_0 \rightarrow {}^7F_2$ transition of the Eu^{3+} ions is an induced-electric-dipole transition and its corresponding intense emission at 615 nm is very sensitive to the coordination environment.[42] This is a very stronge $^5D_0 \rightarrow {}^7F_2$ peak, pointing to a highly polarizable chemical environment around the Eu^{3+} ion, and is responsible for the brilliant-red emission color of these complexes. The most intensity ratio values $\eta(^5D_0 \rightarrow {}^7F_2/{}^5D_0 \rightarrow {}^7F_1)$ of Eu−L−P, Eu−L−P gel, PMMA−Eu−L−P gel, PVP−Eu−L−P gel, and PVB−Eu−L−P gel are 2.9, 4.7, 5.0, 5.2, and 5.2, which indicates the increased departure from symmetry of the coordination environment around the central Eu^{3+} ions and the invoked polarizability effects during the formation of the hybrid materials. The content of the complexes in hybrid materials and its relative luminescence intensity compared with the complex ($^5D_0 \rightarrow {}^7F_2$) are listed in Table 1. It can be seen clearly that the complex of a unit mass in the silica/polymer matrix can give stronger luminescence than the corresponding pure complex. Compared with the complex, the unit mass luminescence intensity (the relative intensity divided by the mass) of the polymer−Eu−L−P gel increases about 2 times. As is known, the photophysical and photochemical processes on guest molecules can be influenced profoundly by an organized matrix. The polymer hybrid matrix, however, is a kind of noncrystalline substance with porous structure (see Figure 6). This

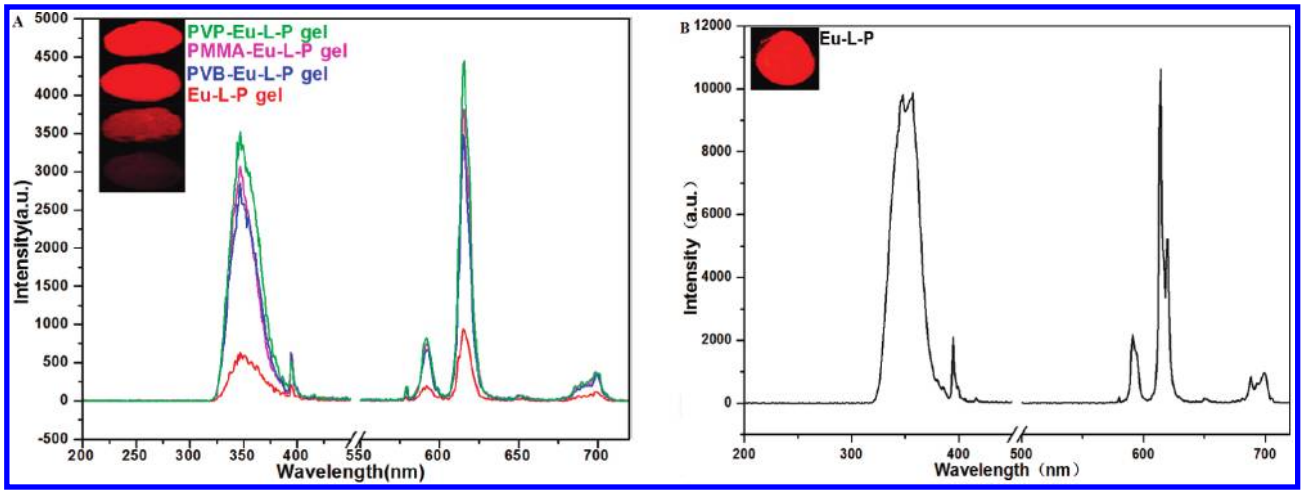

Figure 8. Excitation (monitored at 615 nm) and emission (monitored at the maximum excited wavelengths which are labeled in the excitation spectra) spectra of the hybrid materials (A) and the isolated complex Eu−L−P (B). The excitation and emission slits are both 0.15 nm. The inset photographs show the samples under UVA irradiation (365 nm).

Table 1. Relationship between Contents of the Eu−L−P and Luminescence Intensities

materials	content of complex (wt %)	relative intensities of $^5D_0 \rightarrow {}^7F_2$	unit mass luminescence intensities
Eu−L−P	100	10630	10630
Eu−L−P gel	23.1	943	4082
PMMA−Eu−L−P gel	17.6	3810	21648
PVP−Eu−L−P gel	17.6	4449	25278
PVB−Eu−L−P gel	17.6	3491	19835

host can provide an interesting microenvironment for the guest molecules. We may deduce that when the complex is embedded in the silica/polymer matrixes, the molecules were confined in micropores and the nonradiative transitions were decreased, and the coordination of Eu^{3+} ions has some influence because of the addition of the polymers, resulting in high luminescence efficiency. Moreover, based on the absorption spectra, silica matrix was found to increase the absorbance of the complex by creasing UV scattering microporous structures. Additionally, compared to the Eu−L−P gel, the relative intensities of all the samples of polymer−Eu−L−P gel have increased evidently. Following the twice increase in unit mass intensities, we may deduce that the Ln^{3+} ions can be protected from the O−H groups on the surface of silica by the polymers and the coordination of the carboxyl groups of the polymers. Furthermore, we may infer that this result of diverse luminescence intensities of materials is caused by the differences between the substitutents of the polymers in these materials, and the quenching effects by O−H groups of PVB brought the appreciably feeble intensity of PVB−Eu−L−P gel.

Luminescence Decay Times (τ) and Emission Quantum Efficiency (η). The luminescence lifetimes and quantum yields, which are two important parameters for the estimation of the efficiency of the emission process of the complexes, have also been determined. The $^5D_0$ emission decay curves were monitored at 615 nm under the excitation wavelength that maximizes the emission intensity. The biexponential decay curves and monoexponential decay curve are observed in the Eu−L−P gel, polymer−Eu−L−P gel, and isolated Eu^{3+} complex, respectively. The fitting data are illustrated in Table 2, including of $^5D_0$ levels of Eu^{3+} ions, the corresponding relative weightings for each species, and the average lifetime $\langle\tau\rangle$.[43] The biexponential decay behavior of the activator is often observed when the excitation energy is transferred from the donors which may be the ligand L or probably via the carbonyl groups from the polymers. The results indicate that more than one kind of symmetrical site of Eu^{3+} ion exists in these solid samples except for the ternary complex Eu−L−P. It could be seen from Table 2 that all the polymer−Eu−L−P gel materials exhibit better luminescent properties than Eu−L−P gel. The shortening lifetimes of Eu−L−P gel (0.937 ms) might be given rise to the quenching of abundant O−H oscillators on the matrix surface to some absorbed Eu−L−P. Following the method described in the literature,[44] $^5D_0$ quantum efficiency (q) of the samples on the basis of the emission spectra and lifetimes can be estimated, and the detailed luminescence data presented above are employed. q expresses how well the radiative process (k_r, estimated according to the reported method,[44] shown in Table 2) is competing with nonradiative processes (k_{nr}) in the depopulation of the $^5D_0$ state:

$$q = \frac{k_r}{k_r + k_{nr}} \tag{1}$$

Since the multiexponential decay curves which are usually observed in solid samples[45−47] can be attributed to the highly heterogeneous environments for the complexes in the solid surfaces, the average lifetime $\langle\tau\rangle$ is calculated for each decay according to[47]

$$\langle\tau\rangle = \frac{\sum A_i\tau_i^2}{\sum A_i\tau_i} \tag{2}$$

where τ_i is the component decay time and A_i is weighed amplitude. We propose that the average lifetime ($\langle\tau\rangle$), radiative transition rate (k_r), and nonradiative transition rate (k_{nr}) may be related through the following equation:

$$k_r + k_{nr} = \frac{1}{\langle\tau\rangle} \tag{3}$$

The values found for q (%), average lifetimes ($\langle\tau\rangle$), radiative decay rate (k_r), and nonradiative decay rate (k_{nr}) for all samples are shown in Table 2. The emission quantum efficiency

Table 2. Photoluminescence Data of Polymer−Eu−L−P Gel and Eu−L−P Gel Samples and Isolated Europium Complex in Solids[a]

	Eu−L−P gel	PMMA−Eu−L−P gel	PVP−Eu−L−P gel	PVB−Eu−L−P gel	Eu−L−P[b]
τ_1 (ms)	0.582 (60.53%[c])	0.769 (63.91%)	0.669 (46.53%)	0.607 (52.24%)	1.653 (100%)
τ_2 (ms)	1.201 (39.47%)	1.571 (36.09%)	1.407 (53.47%)	1.227 (47.76%)	
$\langle\tau\rangle$ (ms)	0.937	1.199	1.191	1.009	1.653
k_r (ms^{-1})	0.378	0.390	0.394	0.378	0.332
k_{nr} (ms^{-1})	0.689	0.444	0.445	0.613	0.272
n_w	0.4	0.1	0.2	0.3	0.0
q (%)	35.4	46.8	46.9	38.1	55.0

[a] The lifetimes (τ), average lifetimes $\langle\tau\rangle$, radiative (k_r) and nonradiative (k_{nr}) decay rates, numbers of water molecules in the first coordination sphere (n_w), and emission quantum efficiency (q) of the $^5D_0$ Eu^{3+} excited state were obtained at room temperature. [b] Value obtained at the excitation of 347 nm. [c] Lifetimes (τ) and corresponding relative weightings.

estimated for Eu−L−P gel (35.4%) is lower than that for Eu−L−P (55.0%), but the quantum efficiencies of the hybrid materials employing organic polymers (PVB (38.1%), PMMA (46.8%), and PVP (46.9%)) are higher than that of Eu−L−P gel (35.4%). From eq 1, it can be seen the value of q mainly depends on two equation values including lifetimes and k_r. If the lifetimes and k_r are large, the quantum efficiency must be high. Therefore, the different compositions of the hybrid materials may have an influence on the luminescence lifetimes and quantum efficiencies. For the different polymers, the lifetimes and the emission quantum efficiencies of PVP−Eu−L−P sol and PMMA−Eu−L−P sol are much higher than those of PVB−Eu−L−P sol, which may be due to the structure of the polymers. The steric effect arising from the long polyvinyl chain of PVP on the surface of the isolated Eu^{3+} complex may contribute to protect the isolated Eu^{3+} complex from O−H oscillators of the matrix surfaces. PVP has a structure of a polyvinyl skeleton with polar groups, where the donated lone pair electrons of both nitrogen and oxygen atoms may occupy orbitals of the Eu^{3+} ion to form the complex. Furthermore, the use of PMMA is also a good strategy for protecting the quenching of O−H oscillators between the Eu−L−P and the matrix surface, in which the carbonyl groups can also impart better compatibility with the isolated Eu^{3+} complex. Unfortunately, the PVB molecular chains possess the hydrophilic group hydroxyl, which may decrease the luminescence efficiency. Even so, compared with the unemploying polymer hybrid, the quantum efficiency of the PVB−Eu−L−P gel is still enhanced.

The coordination water molecules produce severe vibration of the hydroxyl group, resulting in a large nonradiative transition and decreasing the luminescence efficiency. The removal of water molecules from the Eu^{3+} coordination sphere after embedding in silica/polymer may be further studied. It is a possibility to estimate the number of water molecules (n_w) coordinated to the Eu^{3+} ions in the silica/polymer hybrid host by using the empirical formula of Supkowski and Horrocks:[48,49]

$$n_w = 1.11(k_{nr} - k_r - 0.31) \quad (4)$$

Agreeing with the assumed formation of the complexes in hybrids, the results (Table 2) indicated that some water molecules in the Eu−L−P gel were removed from the Eu^{3+} first coordination shell after the addition of polymers. The coordination number of water molecules can be arranged in the order Eu−L−P gel > PVB−Eu−L−P gel > PVP−Eu−L−P gel > PMMA−Eu−L−P gel, which is in agreement with the increasing order of the quantum efficiencies.

Stability Studies. *Photoluminescence Stability.* To compare photoluminescence stability, kinetic scans of luminescence induced by UV light (347 nm) for the different samples were carried out. Figure 9 illustrates the normalized emission intensity of the $^5D_0 \rightarrow {}^7F_2$ transition (615 nm) on irradiation times for the different samples. The declining tendencies of the emission intensities of the $^5D_0 \rightarrow {}^7F_2$ transition with increasing exposure time are observed in Eu−L−P gel, polymer−Eu−L−P gel, and isolated Eu^{3+} complex. It is understandable that the decay curve for polymer−Eu−L−P gel presents higher stability than that for Eu−L−P gel because of the shielding effect of the polymers around the embedded Eu^{3+} complexes. It is interesting to observe that the intensities of some hybrid materials actually present higher stabilities than the isolated Eu^{3+} complex with the change of exposure time. We speculated that the matrixes may provide rigid environments for the pure complexes to reduce the energy consumption of vibrations of ligands and intermolecular collisions of complexes.

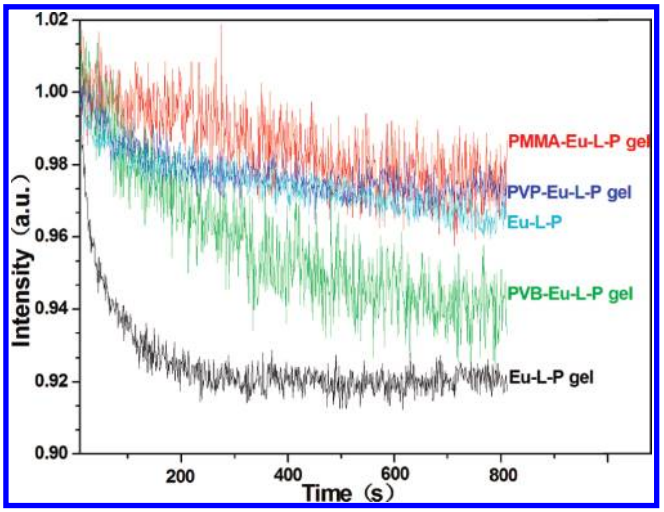

Figure 9. Photoluminescence stabilities of polymer−Eu−L−P gel, Eu−L−P gel, and isolated Eu^{3+} complex Eu−L−P (normalized intensities of the $^5D_0 \rightarrow {}^7F_2$ transition as a function of time).

Thermal Stability. The thermal stabilities of Eu−L−P gel, polymer−Eu−L−P gel, and the isolated Eu−L−P complex were further studied by TG and differential thermogravimetric (DTG) measurements. As the DTG curves show (Figure S2 in the Supporting Information), the thermal stability of the isolated complex (324 °C for Eu−L−P decomposition) is enhanced by loading in Eu−L−P gel (430 °C). It can be seen from TG curve of PMMA−Eu−L−P gel that PMMA began to decompose at 354 °C[50] (314 °C for PVP[50,51] and 312 °C for PVB[33]). When the temperature reached 439 °C (386 °C for PVP and 376 °C for PVB),

the polymer PMMA had departed from the hybrid material completely. In addition, the hybrid material lost mass at the fastest speed when the temperature climbed to 371 °C (358 °C for PVP and 350 °C for PVB), which was observed from the DTG curve with the sharpest peak. The decomposition temperatures of the complexes were 512, 500, and 521 °C for the hybrid materials PMMA−Eu−L−P gel, PVP−Eu−L−P gel, and PVB−Eu−L−P gel, respectively. The results revealed that the thermal stability of the complex was enhanced by loading in the hybrid materials. Generally, the thermal stability of the hybrid material was higher than that of the pure organic complex because of the molecular level hybridization between the rigid silica matrix and the organic complex. In the present study, the thermal stability of the complex was still enhanced after the addition of the polymers into Eu−L−P gel. This kind of material could remain steady below 350 °C, which could be satisfied with current applications in many areas.

CONCLUSIONS

In summary, a series of transparent homogeneous hybrid materials polymer−Eu−L−P gel embedded with a new europium ternary complex were successfully assembled. The microstructures of the obtained hybrid materials have been characterized by FTIR, XRD, SEM, and UV−vis absorption spectra, and the results reveal that the hybrid materials show regular microstructures. The luminescence efficiency and coordinated waters of the Eu^{3+} complex for the hybrid materials and their stabilities under heat or UV light were also studied. As the data suggested, the hybrid materials polymer−Eu−L−P gel in comparison with Eu−L−P gel generally resulted in more efficient emission, and also possessed much higher thermal stability and exposure durability, since the polymers interacted with europium complexes. We deduce that the polymers may also act as antenna, absorbing and transferring energy to the excited energy levels of the central Eu^{3+} ions, with the ensuing enhancement of the luminescence intensities of the novel systems. Because the PVB molecular chain has the hydrophilic group hydroxyl, it is expected that, in the hybrid materials PMMA−Eu−L−P gel and PVP−Eu−L gel, the quantum efficiency of Eu^{3+} ions could be improved over that of the PVB−Eu−L−P gel. In a word, the hybrid materials doped with polymers bring out significant photophysical properties and stabilities. These kinds of homogeneous hybrid polymeric materials can be expected to have potential and significant applications in optical and electronic devices in the future.

ASSOCIATED CONTENT

Supporting Information. The ^1H NMR data of the ligand H_2L, the crystal data and details of the structure determination for the ternary complex Eu−L−P, FTIR spectra, TG and DTG curves of polymer−Eu−L−P gel samples. CCDC 785155 contains the supplementary crystallographic data for this paper. This material is available free of charge via the Internet at http://pubs.acs.org. These data can be obtained free of charge from the Cambridge Crystallographic Data Centre via http://www.ccdc.cam.ac.uk/cgi-bin/catreq.cgi.

AUTHOR INFORMATION

Corresponding Author

*Telephone: +86-931-8912552. Fax: +86-931-8912582. E-mail: tangyu@lzu.edu.cn.

ACKNOWLEDGMENT

We are grateful to the National Natural Science Foundation of China (Project 20931003, 21071068) and the program for New Century Excellent Talents in University (NCET-06-0902) for financial support.

REFERENCES

(1) Binnemans, K. *Chem. Rev.* **2009**, *109*, 4283–4374.
(2) Carlos, L. D.; Ferreira, R. A. S.; de Zea Bermudez, V.; Ribeiro, S. J. L. *Adv. Mater.* **2009**, *21*, 509–534.
(3) Martínez-Máñez, R; Sancenón, F. *Chem. Rev.* **2003**, *103*, 4419–4476.
(4) Bünzli, J.-C. G.; Piguet, C. *Chem. Rev.* **2002**, *102*, 1897–1928.
(5) Yang, X. P.; Jones, R. A.; Oye, M. M.; Holmes, A. L.; Wong, W.-K. *Cryst. Growth Des.* **2006**, *6*, 2122–2125.
(6) Tang, Y.; Tang, K.-Z.; Zhang, J.; Su, C.-Y.; Liu, W.-S.; Tan, M.-Y. *Inorg. Chem. Commun.* **2005**, *8*, 1018–1021.
(7) Brotin, T.; Dutasta, J.-P. *Chem. Rev.* **2009**, *109*, 88–130.
(8) Burdinski, D.; Pikkemaat, J. A.; Lub, J.; de Peinder, P.; Garrido, L. N.; Weyhermüller, T. *Inorg. Chem.* **2009**, *48*, 6692–6712.
(9) Morrow, J. R.; Amyes, T. L.; Richard, J. P. *Acc. Chem. Res.* **2008**, *41*, 539–548.
(10) Wang, Q.; Tang, K.-Z.; Liu, W.-S.; Tang, Y.; Tan, M.-Y. *J. Solid State Chem.* **2009**, *182*, 3118–3124.
(11) Stich, M. I. J.; Nagl, S.; Wolfbeis, O. S.; Henne, U.; Schaeferling, M. *Adv. Funct. Mater.* **2008**, *18*, 1399–1406.
(12) Fernandes, M.; de Zea Bermudez, V.; Sá Ferreira, R. A.; Carlos, L. D.; Charas, A.; Morgado, J.; Silva, M. M.; Smith, M. J. *Chem. Mater.* **2007**, *19*, 3892–3900.
(13) Mackenzie, J. D.; Bescher, E. P. *Acc. Chem. Res.* **2007**, *40*, 810–818.
(14) Velasco, D. S.; de Moura, A. P.; Medina, A. N.; Baesso, M. L.; Rubira, A. F.; Cremona, M.; Bento, A. C. *J. Phys. Chem. B* **2010**, *114*, 5657–5660.
(15) Lenaerts, P.; Storms, A.; Mullens, J.; D'Haen, J.; Görller-Walrand, C.; Binnemans, K.; Driesen, K. *Chem. Mater.* **2005**, *17*, 5194–5201.
(16) Wada, Y.; Sato, M.; Tsukahara, Y. *Angew. Chem., Int. Ed.* **2006**, *45*, 1925–1928.
(17) Gago, S.; Fernandes, J. A.; Rainho, J. P.; Sá Ferreira, R. A.; Pillinger, M.; Valente, A. A.; Santos, T. M.; Carlos, L. D.; Ribeiro-Claro, P. J. A.; Gonçalves, I. S. *Chem. Mater.* **2005**, *17*, 5077–5084.
(18) Yan, B.; Wang, Q.-M. *Cryst. Growth Des.* **2008**, *8*, 1484–1489.
(19) Brunet, E.; Alhendawi, H. M. H.; Juanes, O.; Jiménez, L.; Rodríguez-Ubis, J. C. *J. Mater. Chem.* **2009**, *19*, 2494–2502.
(20) Terazzi, E.; Suarez, S.; Torelli, S.; Nozary, H.; Imbert, D.; Mamula, O.; Rivera, J. P.; Guillet, E.; Bénech, J. M.; Bernardinelli, G.; Scopelliti, R.; Donnio, B.; Guillon, D.; Bünzli, J. C. G.; Piguet, C. *Adv. Funct. Mater.* **2006**, *16*, 157–168.
(21) Pumera, M.; Cabala, M.; Veltruská, K.; Ichinose, I.; Tang, J. *Chem. Mater.* **2007**, *19*, 6513–6517.
(22) Lezhnina, M.; Benavente, E.; Bentlage, M.; Echevarría, Y.; Klumpp, E.; Kynast, U. *Chem. Mater.* **2007**, *19*, 1098–1102.
(23) Xu, Z.; Kang, X.; Li, C.; Hou, Z.; Zhang, G.; Yang, D.; Li, G.; Lin, J. *Inorg. Chem.* **2010**, *49*, 6706–6715.
(24) Wang, Q.; Tan, C.; Chen, H.; Tamiaki, H. *J. Phys. Chem. C.* **2010**, *114*, 13879–13883.
(25) Pénard, A.-L.; Gacoin, T.; Boilot, J.-P. *Acc. Chem. Res.* **2007**, *40*, 895–902.
(26) Lin, J.; Yu, M.; Lin, C. K.; Liu, X. M. *J. Phys. Chem. C* **2007**, *111*, 5835–5845.
(27) Sun, L. N.; Zhang, H. J.; Meng, Q. G.; Liu, F. Y.; Fu, L. S.; Peng, C. Y.; Yu, J. B.; Zheng, G. L.; Wang, S. B. *J. Phys. Chem. B* **2005**, *109*, 6174–6182.
(28) Sanchez, C.; Boissière, C.; Grosso, D.; Laberty, C.; Nicole, L. *Chem. Mater.* **2008**, *20*, 682–737.

(29) Dang, S.; Sun, L.-N.; Zhang, H.-J.; Guo, X.-M.; Li, Z.-F.; Feng, J.; Guo, H.-D.; Guo, Z.-Y. *J. Phys. Chem. C* **2008**, *112*, 13240–13247.
(30) Zhang, D. J.; Wang, X. M.; Qiao, Z. A.; Tang, D. H.; Liu, Y. L.; Huo, Q. S. *J. Phys. Chem. C* **2010**, *114*, 12505–12510.
(31) Bekiari, V.; Lianos, P. *J. Sol-Gel Sci. Technol.* **2003**, *26*, 887–890.
(32) Nakajima, H.; Kawano, K. *J. Alloys Compd.* **2006**, *408*−*412*, 701–705.
(33) Elias, H. G. *An Introduction to Polymer Science*: VCH: Weinheim, Germany, 1997.
(34) Van der Made, A. W.; Van der Made, R. H. *J. Org. Chem.* **1993**, *58*, 1262–1263.
(35) *SMART*, edition 5.05; Bruker AXS, Inc.: Madison, WI, 1998.
(36) *Bruker Advanced X-ray Solutions SAINT*, version 6.45; Bruker AXS, Inc.: Madison, WI, 1997−2003.
(37) Sheldrick, G. M. *SADABS: Area-Detector Absorption Correction*; University of Göttingen: Göttingen, Germany, 1996.
(38) Sheldrick, G. M. *SHELXL-97, Program for the Refinement of Crystal Structures*; University of Göttingen: Göttingen, Germany, 1997.
(39) Oliveira, D. C.; Macedo, A. G.; Silva, N. J. O.; Molina, C.; Ferreira, R. A. S.; André, P. S.; Dahmouche, K.; Bermudez, V. D. Z.; Messaddeq, Y.; Ribeiro, S. J. L.; Carlos, L. D. *Chem. Mater.* **2008**, *20*, 3696–3705.
(40) Balamurugan, A.; Reddy, M. L. P.; Jayakannan, M. *J. Phys. Chem. B* **2009**, *113*, 14128–12138.
(41) Wan, C. Y.; Li, M.; Bai, X.; Zhang, Y. *J. Phys. Chem. C* **2009**, *113*, 16238–16246.
(42) Posati, T.; Bellezza, F.; Cipiciani, A.; Costantino, F.; Nocchetti, M.; Tarpani, L.; Latterini, L. *Cryst. Growth Des.* **2010**, *10*, 2847–2850.
(43) Martínez, V. M.; Arbeloa, F. L.; Prieto, J. B.; Arbeloa, I. L. *J .Phys. Chem. B* **2005**, *109*, 7443–7450.
(44) Martinus, H.; Werts, V.; Ronald, Y.; Jukes, T. F.; Verhoeven, J. W. *Phys. Chem. Chem. Phys.* **2002**, *4*, 1542–1548.
(45) Wen, X.; Li, M.; Wang, Y.; Zhang, J.; Fu, L.; Hao, R.; Ma, Y.; Ai, X. *Langmuir* **2008**, *24*, 6932–6936.
(46) Hagerman, M. E.; Salamone, S. J.; Herbst, R. W.; Payeur, A. L. *Chem. Mater.* **2003**, *15*, 443–450.
(47) Martínez Martínez, V.; López Arbeloa, F.; Bañuelos Prieto, J.; López Arbeloa, I. *J. Phys. Chem. B* **2005**, *109*, 7443–7450.
(48) Supkowski, R. M.; Horrocks, W. D. *Inorg. Chim. Acta* **2002**, *340*, 44–48.
(49) Tiseanu, C.; Parvulescu, V. I.; Kumke, M. U.; Dobroiu, S.; Gessner, A.; Simon, S. *J. Phys. Chem. C* **2009**, *113*, 5784–5791.
(50) Zhang, H.; Song, H.-W.; Dong, B.; Han, L.-L.; Pan, G.-H.; Bai, X.; Fan, L.-B.; Lu, S.-Z.; Zhao, H.-F.; Wang, F. *J. Phys. Chem. C* **2008**, *112*, 9155–9162.
(51) Sukpirom, N.; Lerner, M. M. *Chem. Mater.* **2001**, *13*, 2179–2185.